Evolutions of anisotropic universe on interacting holographic and new agegraphic scalar fields models of dark energy

Hossien Hossienkhani[1,*] and Ali Aghamohammadi[2,†]

[1]*Hamedan Branch, Islamic Azad University, Hamedan, Iran*
[2]*Sanandaj Branch, Islamic Azad University, Sanandaj, Iran*

(Dated: February 3, 2017)

arXiv:1602.07683v3 [gr-qc] 2 Feb 2017

Abstract

A spatially homogeneous and anisotropic Bianchi type I universe has been studied with the interacting holographic and new agegraphic scalar fields models of dark energy. Given, the framework of the anisotropic model, both the dynamics and potential of these scalar field models according to the evolutionary behavior of both dark energy models are reconstructed. We also investigate the cosmological evolution of interacting dark energy models, and compare it with observational data and schematic diagram. In order to do so, we focus on observational determinations of the expansion history $H(z)$. Next, we evaluate effects of anisotropy on various topics, such as evolution of the growth of perturbations in the linear regime, statefinder diagnostic, Sandage-Loeb (SL) test and distance modulus from holographic and new agegraphic dark energy models and compare the results with standard FRW and ΛCDM and wCDM models. Our numerical result show the effects of the interaction and anisotropy on the evolutionary behavior the new agegraphic scalar field models.

keywords: Anisotropic universe; Statefinder diagnostic; Sandage-Loeb test; Holographic dark energy; New agegraphic; Scalar field

I. INTRODUCTION

Most remarkable observational discoveries in type-Ia supernovae (SN Iae) prevail that the universe has confirmed by two dark components containing dark energy (DE) and dark matter (DM) [1, 2]. DE, an unknown energy with large negative pressure, is utilized to explain the present cosmic accelerating expansion of the universe. The simplest candidate for DE is Einstein's cosmological constant (Λ) which is equivalent to the vacuum energy density in the universe and produces negative pressure with equation of state (EoS) parameter $\omega_\Lambda = -1$ since it fits the observational data well, but it suffers two well-known problems, i.e., "fine tuning problem" and "cosmic coincidence problem".
Recently, considerable interest has been stimulated in explaining the observed DE by the holographic dark energy (HDE) model. It is well known that the holographic principle is an emergent result of the recent studies for exploring the quantum gravity [3–5]. According to the holographic principle, the entropy of a system scales not with its volume, but with its surface area [6]. The HDE was first proposed in [7] following the line of [8] where the infrared cut-off is taken to be the size of event horizon for DE. Ref. [8] purposed that the DE should obey this principle, thus its energy density has an upper limit and the fin-tuning problem for the cosmological constant is omitted. Its framework is the black hole thermodynamics [9] and the correspondence of the UV cut-of of a quantum field theory, which gives rise to the vacuum energy, with the distance of the theory [10, 11]. Li [7] and Hsu [12] formulated the acquired vacuum energy as HDE i.e. $\rho_\Lambda = 3c^2L^{-2}$, where c is a numerical constant and L is the infrared cutoff. If in a cosmological context we saturate this inequality by doing $L = H^{-1}$ [13], where H is the Hubble parameter, we obtain a model of holographic nature for the density of DE. Ref. [14] was presented a generalized and restored HDE in the braneworld context. The holographic phantom energy density grows rapidly and dominates the late time expanding phase, helping realize a cyclic universe scenario in Ref. [15].
Another plan to explore the nature of DE, dubbed agegraphic DE (ADE), has been proposed [16] which explain the acceleration of the universe expansion with the gravitational effect in general relativity. In the ADE models the age of the universe is taken the length measure instead of the horizon distance, so the causality problem that appears in the HDE model can be avoided [17]. After introducing the ADE model by Cai [16], a new model of agegraphic DE

*Electronic address: hossienhossienkhani@yahoo.com
†Electronic address: a.aqamohamadi@gmail.com,or,a.aghamohamadi@iausdj.ac.ir

(NADE) was proposed in Ref. [18], while the time scale is chosen to be the conformal time η instead of the age of the universe i.e. T. The ADE undergo from the difficulty to characterize the matter dominated era [18] while the NADE resolved this subject [19]. Many authors did some detailed study of this NADE model [20–24].
A Bianchi type I (BI) universe, being the straightforward generalization of the flat FRW universe, is of interest because it is one of the simplest models of a non-isotropic universe exhibiting a homogeneity and spatial flatness. In this case, unlike the FRW universe which has the same scale factor for three spatial directions, a BI universe has a different scale factor for each direction. This fact introduce a non-isotropy to the system. The possible effects of anisotropy in the early universe have been investigated with BI models from different points of view [25–28]. Therefore, we establish a correspondence between the interacting holographic and new agegraphic DE scalar field in an anisotropic universe. The organisation of this work is as follows. In the next section, a brief review of the general formulation of the field equations in a BI metric are discussed, then, interacting DE with cold DM (CDM) in a non-isotropic BI universe is studied. The Sec. III is concerned with interacting HDE with the quintessence, tachyon and K-essence scalar field in an anisotropic universe. The Sec. IV, is related to establish the correspondence between the model of interacting NADE and the quintessence, tachyon and K-essence DE in BI model. In Sec. V we study effects of anisotropy on the $H(z)$ data, SL test, the statefinder diagnostic, the linear evolution of perturbations and distance modulus with both HDE and NADE models and compares it with the ΛCDM, wCDM and FRW models. At last the Sec. VI is devoted to conclusion and discussion.

II. GENERAL FRAMEWORK

Bianchi cosmologies are spatially homogeneous but not necessarily isotropic. Here we will consider BI cosmology. The metric of this model is given by

$$ds^2 = dt^2 - A^2(t)dx^2 - B^2(t)dy^2 - C^2(t)dz^2, \tag{1}$$

where the metric functions, A, B, C, are merely functions of time, t. However, the underlying Lie algebra of the isometry group of the BI metrics is completely different [29]. The contribution of the interaction with the matter fields is given by the energy momentum tensor, which is defined as

$$T^{\mu}_{\nu} = diag[\rho, -\omega\rho, -\omega\rho, -\omega\rho], \tag{2}$$

where ρ and ω represent the energy density and EoS parameter, respectively. The field equations for the axially symmetric BI metric are [30–32]:

$$3H^2 - \sigma^2 = \frac{1}{M_p^2}(\rho_m + \rho_\Lambda), \tag{3}$$

$$3H^2 + 2\dot{H} + \sigma^2 = -\frac{1}{M_p^2}\left(p_m + p_\Lambda\right), \tag{4}$$

where $M_p^2 = 1/(8\pi G)$, ρ_Λ and p_Λ are the Planck mass, the energy density and pressure of DE, respectively, and $a = (ABC)^{\frac{1}{3}}$ is the scale factor, and $\sigma^2 = 1/2\sigma_{ij}\sigma^{ij}$ in which $\sigma_{ij} = u_{i,j} + \frac{1}{2}(u_{i;k}u^k u_j + u_{j;k}u^k u_i) + \frac{1}{3}\theta(g_{ij} + u_i u_j)$ is the shear tensor ($\sigma_{ij}u^j = 0, \sigma^i{}_i = 0$), which describes the rate of distortion of the matter flow, and $\theta = 3H = u^j_{;j}$ is the scalar expansion, where u^j is 4-velocity. In a comoving coordinate system, i.e. ($u^i = \delta^i_0$). From the metric Eq. (1), and considering the comoving frame, we find that the components of the average Hubble parameter and the shear tensor are given by

$$H = \frac{1}{3}(\frac{\dot{A}}{B} + \frac{\dot{B}}{B} + \frac{\dot{C}}{C}), \tag{5}$$

$$\sigma^2 = 3H^2 - (\frac{\dot{A}\dot{B}}{AB} + \frac{\dot{B}\dot{C}}{BC} + \frac{\dot{A}\dot{C}}{AC}), \tag{6}$$

By using Eq. (3), the dimensionless density parameter of BI can also be defined as usual

$$\Omega_m = \frac{\rho_m}{\rho_{cr}}, \quad \Omega_\Lambda = \frac{\rho_\Lambda}{\rho_{cr}}, \tag{7}$$

where the critical energy density is $\rho_{cr} = 3M_p^2H^2$. Using Eq. (7), we can rewrite (3) in the form of fractional energy densities as

$$\Omega_m + \Omega_\Lambda = 1 - \frac{\sigma^2}{3H^2}. \tag{8}$$

The above equation shows that the sum of the energy density parameters approaches 1 at late times. So at late times the universe becomes flat. Therefore for sufficiently large time, this model predicts that the anisotropy of the universe will damp out and universe will become isotropic. This result also shows that in the early universe i.e. during the radiation and matter dominated era the universe was anisotropic and the universe approaches to isotropy as DE starts to dominate the energy density of the universe. When isotropic is assumed, $\Omega_m + \Omega_\Lambda = 1$, and the model has only one free parameter, Ω_Λ. We shall take that the shear scalar can be described based on the average Hubble parameter, $\sigma^2 = \sigma_0^2 H^2$, where σ_0^2 is a constant. So, Eq. (8) lead to

$$\Omega_m + \Omega_\Lambda = 1 - \Omega_{\sigma 0}, \quad with \;\; \Omega_{\sigma 0} = \frac{\sigma_0^2}{3}, \tag{9}$$

where $\Omega_{\sigma 0}$ is the anisotropy parameter. We assume that the DE is coupled with DM, in such way that total energy-momentum is still conserved. In the flat BI cosmology with a scale factor a, the continuity equations for both components are [33]

$$\dot{\rho}_\Lambda + 3H\rho_\Lambda(1+\omega_\Lambda) = -Q, \tag{10}$$

$$\dot{\rho}_m + 3H\rho_m = Q, \tag{11}$$

where $\omega_\Lambda = p_\Lambda/\rho_\Lambda$ is the EoS parameter of the interacting DE and Q is the interaction term. The case $Q > 0 (Q < 0)$ corresponds to either DE transformation into DM and vice versa of the model. Following [10, 11], we shall assume $Q = 3b^2H(\rho_m + \rho_\Lambda)$ with the coupling constant b^2. In the following, we will find a form for the function $V(\phi)$, which is able to reconstruct HDE and NADE models as following.

III. HDE WITH HUBBLE RADIUS AS IR CUTOFF IN BI MODEL

First we will consider the size L as the Hubble radius H^{-1}, thus the energy density for the DE becomes [3, 34, 35]

$$\rho_\Lambda = 3c^2 M_p^2 H^2, \tag{12}$$

where c^2 is a constant. As it is well known, different possibilities have been tried to varying degrees of success, namely, the particle horizon [36], the future event horizon [7, 10] and the Hubble horizon [13]. Hence, we set the Hubble radius as the infrared cutoff $L = H^{-1}$ [37]. It can be seen that the problem of taking Hubble radius, the DE results as pressureless, since ρ_Λ scales like matter energy density ρ_m with the scale factor a as a^{-3}, therefore producing a decelerated expansion. At this point our system of equations is not closed and we still have freedom to choose. In order to accelerate the universe more, we have added the interaction as well as anisotropy, as it can be seen in equation (14). This is a new model to explore the physical mechanism responsible for the current acceleration of the universe. Therefor in the present work, we have tried to compensate the effects, (due to the Hubble's first radius that lead to a deceleration of the universe) using interaction and anisotropy. For $b^2 = \Omega_{\sigma 0} = 0$ and this result is consistent with the Refs. [12, 35, 37–39]. Now by taking the time derivative of relation (12) and using the BI equation we find

$$\dot{\rho}_\Lambda = 2\rho_\Lambda \frac{\dot{H}}{H} = -3\frac{Hc^2\rho_\Lambda}{1-\Omega_{\sigma 0}}(1+\omega_\Lambda + r), \tag{13}$$

where $r = \rho_m/\rho_\Lambda = (1-\Omega_{\sigma 0}-\Omega_\Lambda)/\Omega_\Lambda$ is the energy density ratio. Substituting Eq. (13) into (10), the EoS parameter for interaction HDE is given by

$$\omega_\Lambda = -\frac{b^2(1-\Omega_{\sigma 0})^2}{c^2(1-c^2-\Omega_{\sigma 0})}. \tag{14}$$

This relation shows that the EoS parameter is depend on b^2, c and $\Omega_{\sigma 0}$ parameter. Therefore, ω_Λ becomes a constant. In the absence of interaction between HDE and CDM, $b^2 = 0$ we have $\omega_\Lambda = 0$, which is that matter dominant. It may be pointed out here that if one sets $\Omega_{\sigma 0} = 0$, Eq. (14) reduce to that obtained for a flat FRW universe [35].
Now, we intend to categorize our study into three types of the model, i.e. quintessence, tachyon and K-essence models in non-isotropic universe.

A. Quintessence reconstruction of HDE in BI

We consider a scalar field (the quintessence field) ϕ, evolving in a potential $V(\phi)$. The density and pressure of quintessence are given by

$$\rho_\phi = \frac{1}{2}\dot{\phi}^2 + V(\phi), \tag{15}$$

$$p_\phi = \frac{1}{2}\dot{\phi}^2 - V(\phi), \tag{16}$$

where $\dot{\phi}^2$ is termed as kinetic energy. Quintessence is usually parameterized by its equation of state $\omega_\phi = p_\phi/\rho_\phi$. Looking at Eqs. (15) and (16), we see immediately that $\omega_\phi \geq -1$. The scalar field potential and the corresponding kinetic energy of the field are obtained from Eqs. (15) and (16), which are

$$V(\phi) = \frac{1-\omega_\phi}{2}\rho_\phi, \tag{17}$$

$$\dot{\phi}^2 = (1+\omega_\phi)\rho_\phi, \tag{18}$$

where $\omega_\phi = p_\phi/\rho_\phi$. For the accelerated expansion of the universe, the EoS parameter for quintessence must be less than $-1/3$. By means of $\rho_\phi = \rho_\Lambda$ and $\omega_\phi = \omega_\Lambda$ and substituting Eqs. (12) and (14) into (18) one can get

$$\phi = cM_p\sqrt{3(1-\frac{b^2(1-\Omega_{\sigma 0})^2}{c^2(1-c^2-\Omega_{\sigma 0})})}\ln a. \tag{19}$$

By using Eqs. (3), (7), (12) and (14) we obtain

$$\frac{\dot{H}}{H^2} = -\frac{3}{2}\left(1-\frac{b^2(1-\Omega_{\sigma 0})}{1-c^2-\Omega_{\sigma 0}}\right). \tag{20}$$

Integration of Eq. (20), the scaler field (19) can be written

$$\phi = \frac{2cM_p}{\sqrt{3}}\frac{\sqrt{1-\frac{b^2(1-\Omega_{\sigma 0})^2}{c^2(1-c^2-\Omega_{\sigma 0})}}}{1-\frac{b^2(1-\Omega_{\sigma 0})}{1-c^2-\Omega_{\sigma 0}}}\ln t, \tag{21}$$

and the potential

$$V(\phi) = \frac{2c^2M_p^2}{3}\left(\frac{1+\frac{b^2(1-\Omega_{\sigma 0})}{1-c^2-\Omega_{\sigma 0}}}{\left(1-\frac{b^2(1-\Omega_{\sigma 0})}{1-c^2-\Omega_{\sigma 0}}\right)^2}\right)exp\left(-\frac{\sqrt{3}\phi}{cM_p}\frac{1-\frac{b^2(1-\Omega_{\sigma 0})}{1-c^2-\Omega_{\sigma 0}}}{\sqrt{1-\frac{b^2(1-\Omega_{\sigma 0})^2}{c^2(1-c^2-\Omega_{\sigma 0})}}}\right). \tag{22}$$

From the solution of (20), it is readily given the scale factor is $a = t^{\frac{2}{3}\left(1-\frac{b^2(1-\Omega_{\sigma 0})}{1-c^2-\Omega_{\sigma 0}}\right)^{-1}}$. It clear that an accelerated universe $b^2 > (1-c^2-\Omega_{\sigma 0})/3(1-\Omega_{\sigma 0})$ can be obtained when $\ddot{a} > 0$.

B. Tachyon reconstruction of HDE in BI

The tachyon model, originated from the string theory, has been suggested to explain DE scenario. It has an interesting feature that a rolling tachyon interpolates the EoS parameter between -1 to 0. Also, the tachyon model is the best candidate for inflation at high energy. In a flat BI background the energy density and the pressure density are given by [40–42]

$$\rho_T = -T_0^0 = \frac{V(\phi)}{\sqrt{1-\dot{\phi}^2}}, \tag{23}$$

$$p_T = T_i^i = -V(\phi)\sqrt{1-\dot{\phi}^2}. \tag{24}$$

The EoS of the tachyon is given by

$$\omega_T = \dot{\phi}^2 - 1. \tag{25}$$

In the following, one can express ϕ in terms of b^2, c^2 and $\Omega_{\sigma 0}$. Hence, by equating (14) with (25), i.e. $\omega_\Lambda = \omega_T$, which gives

$$\phi(t) = \sqrt{1 - \frac{b^2(1-\Omega_{\sigma 0})^2}{c^2(1-c^2-\Omega_{\sigma 0})}}t. \tag{26}$$

Integrating of Eq. (20) and using (26) we obtain tachyon potential in term of the scalar field

$$V(\phi) = \frac{4M_p^2 cb(1-\Omega_{\sigma 0})}{3\phi^2\sqrt{1-c^2-\Omega_{\sigma 0}}} \frac{1 - \frac{b^2(1-\Omega_{\sigma 0})^2}{c^2(1-c^2-\Omega_{\sigma 0})}}{(1 - \frac{b^2(1-\Omega_{\sigma 0})}{1-c^2-\Omega_{\sigma 0}})^2}. \tag{27}$$

In this case the evolution of the tachyon is as $\phi \propto t$. Tachyon potentials, which are not steep compared to $V(\phi) \propto \phi^{-2}$ lead to an accelerated expansion [43].

C. K-essence reconstruction of HDE in BI

The K-essence model is different from quintessence scalar field model in the sense that it evolves the universe in the accelerated expansion era. It is originated from the idea of K-inflation which was used to describe the inflation of the early universe at high energies [44]. This kind of models is characterized by non-canonical kinetic energy terms, and are described by a general scalar field action, which is a function of ϕ and $\chi = \dot{\phi}^2/2$, and is given by [45]

$$S = \int d^4x\sqrt{-g}P(\phi,\chi), \tag{28}$$

where $P(\phi,\chi)$ is an arbitrary function of ϕ and its kinetic energy χ. Based on the analysis of the Lagrangian density, it can be transformed into

$$P(\phi,\chi) = f(\phi)(-\chi + \chi^2), \tag{29}$$

and the energy density in these models is given by

$$\rho(\phi,\chi) = f(\phi)(-\chi + 3\chi^2). \tag{30}$$

And the EoS parameter $\omega_K = P(\phi,\chi)/\rho(\phi,\chi)$ is

$$\omega_K = \frac{\chi - 1}{3\chi - 1}. \tag{31}$$

This shows that ω_K does not change for the fix χ. Equating $\omega_K = \omega_\Lambda$ from Eq. (14) and (31), we get

$$\chi = \frac{b^2(1-\Omega_{\sigma 0})^2 + c^2(1-c^2-\Omega_{\sigma 0})}{3b^2(1-\Omega_{\sigma 0})^2 + c^2(1-c^2-\Omega_{\sigma 0})}. \tag{32}$$

The EoS parameter in Eq. (31) diverges for $\chi = 1/3$. For the case of $\chi > 1/3$, the condition $\omega_K < -1/3$ leads to a high bound on $\chi < 2/3$. The requirement of an accelerated expansion gives $1/3 < \chi < 2/3$ and the cosmological constant limit corresponds to $\chi = 1/2$. As we have demanded that the EoS parameter be positive, Eq. (31) implies that $\chi - 1 < -2/3 < 0$. Using Eq. (32) and $\chi = \dot{\phi}^2/2$, one can write the equation for the K-essence field as follows

$$\phi(t) = \sqrt{2\frac{b^2(1-\Omega_{\sigma 0})^2 + c^2(1-c^2-\Omega_{\sigma 0})}{3b^2(1-\Omega_{\sigma 0})^2 + c^2(1-c^2-\Omega_{\sigma 0})}}t, \tag{33}$$

Note that the field increases with the increment of t. From Eqs. (30) and (32) it can be obtained an expression for the k-essence potential $f(\phi)$ in terms of the ϕ

$$f(\phi) = \frac{4M_p^2}{3\phi^2}\frac{3b^2(1-\Omega_{\sigma 0})^2 + c^2(1-c^2-\Omega_{\sigma 0})}{1-c^2-\Omega_{\sigma 0}-b^2(1-\Omega_{\sigma 0})}, \tag{34}$$

where Eq. (31) was used. From Eq. (33) we see that the kinetic energy of K-essence is not constant and is variable with cosmic time.

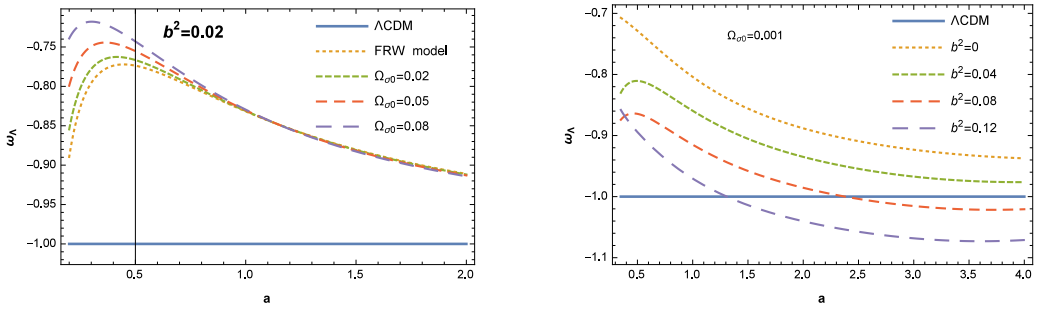

FIG. 1: The plot shows the evolution of the EoS parameter of NADE, Eq. (39), for different the anisotropy energy density parameter $\Omega_{\sigma 0}$ and the coupling constant b^2. For both cases, we take $n = 2.886$ and $\Omega_\Lambda^0 = 0.72$.

IV. NADE WITH SCALAR FIELD IN BI MODEL

The energy density of the NADE can be written

$$\rho_\Lambda = \frac{3n^2 M_p^2}{\eta^2}, \tag{35}$$

where the numerical factor $3n^2$ has been introduced to parameterize some uncertainties, such as the species of quantum fields in the universe, or the effect of curved space-time. The conformal time is given by

$$\eta = \int \frac{dt}{a(t)} = \int \frac{da}{Ha^2}. \tag{36}$$

If we write η to be a definite integral, there will be an integral constant in addition. Thus, we have $\dot{\eta} = 1/a$. The energy density parameter of the NADE is now given by

$$\Omega_\Lambda = \frac{n^2}{H^2\eta^2}. \tag{37}$$

Taking the derivative of Eq. (35) with respect to the cosmic time and using (37) we get

$$\dot{\rho}_\Lambda = -2H\frac{\sqrt{\Omega_\Lambda}}{na}\rho_\Lambda. \tag{38}$$

Inserting this relation into (10) we obtain the EoS parameter of the interacting NADE

$$\omega_\Lambda = -1 + \frac{2}{3na}\sqrt{\Omega_\Lambda} - \frac{b^2}{\Omega_\Lambda}(1 - \Omega_{\sigma 0}). \tag{39}$$

It is important to note that when $b^2 = 0$, the interacting DE becomes trivial and Eq. (39) reduces to its respective expression in new ADE in general relativity [30]. In this case ($b^2 = 0$), the present accelerated expansion of our universe can be derived only if $n > 1$ [18], in addition, we see that the EoS parameter translates the universe from vacuum DE region towards quintessence region; eventually, for the case of matter dominated era $\omega_\Lambda = -2/3$ whilst $\Omega_\Lambda = n^2a^2/4$ and in the radiation dominated era $\omega_\Lambda = -1/3$ whilst $\Omega_\Lambda = n^2a^2$. We test this scenario for the interaction between NADE and DM by using some observational results. For the comparison with the phenomenological interacting model, in our scenario the coupling between NADE and DM can be expressed by b^2 parameter as in the phenomenological interaction form. In fact, b^2 is within the region of the golden supernova data fitting result $b^2 = 0.00^{+0.11}_{-0.00}$ [10] and the observed CMB low l data constraint [46]. In figure 1 we plot the evolution behaviors of EoS ω_Λ of DE, with respect to different choices of anisotropy energy density parameter $\Omega_{\sigma 0}$ and interaction parameter b^2 and the ΛCDM model. It clear that the EoS parameter decrease with the scale factor increase and the effect of various $\Omega_{\sigma 0}$ are negligible but as $a \to 0$, it is clear that increasing of the $\Omega_{\sigma 0}$ cause to increase the EoS parameter. Notice that in the case of $b^2 \geq 0.08$, ω_Λ crosses the phantom divide line $\omega_\Lambda = -1$. Another best fit data with the NADE model is $n = 2.886^{+0.084}_{-0.082}$ at the 1σ level and $n = 2.886^{+0.169}_{-0.163}$ at the 2σ level [24], $n = 2.807^{+0.087}_{-0.086}(1\sigma)^{+0.176}_{-0.170}(2\sigma)$ [47], for using the SNIa data, it is $n = 2.954^{+0.264}_{-0.245}$ at 1σ Confidence Level and $n = 2.716^{+0.111}_{-0.109}$ with SNIa, CMB and Large Scale Structure data [19]

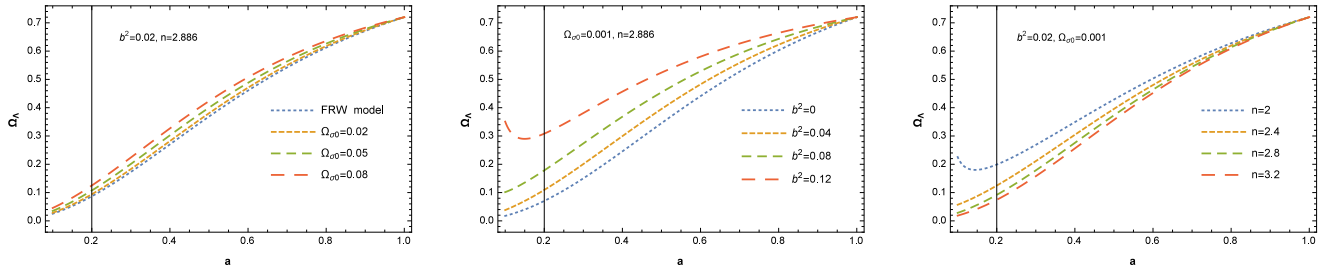

FIG. 2: Left figure representations of Ω_Λ for the NADE with a for different value of the $\Omega_{\sigma 0}$, middle panel representations of Ω_Λ for different value of the b^2 and right panel representations of Ω_Λ for various model parameters n . The initial data is same as in Fig. (1).

and for the non-flat universe $n = 2.673^{+0.053+0.127+0.199}_{-0.077-0.151-0.222}$ [48]. For the ΛCDM cosmology, $\Omega_{m0} = 0.274$ is given by the WMAP five-year observations [25]. In what follows given to the Eq. (39) and its evaluations in the Fig. (1), by pick $b^2 \neq 0$, taking account $\Omega_{m0} = 0.274$ [25], $\Omega_{\Lambda 0} = 1 - (\Omega_{m0} + \Omega_{\sigma 0})$, $\Omega_{\sigma 0} = 0.001$, $n = 2.7$ [19] and $a = 1$ for the present time, Eq. (39) gives

$$\omega_\Lambda = -0.7905 - 1.3875 b^2, \tag{40}$$

where is clear that the phantom EoS $\omega_\Lambda < -1$ can be achieved by set $b^2 > 0.15$ for the coupling between NADE and CDM. In the future, where $a \to \infty$, $\omega_\Lambda < -1$ for $b^2 > 0$, i.e. it may be the ω_Λ crosses the phantom divide line in the presence interacting DM and DE. We can also obtain the evolution behavior of the dark energy. Taking the time derivative of Ω_Λ in Eq. (37) and relation $\dot{\Omega}_\Lambda = H\Omega'_\Lambda$, give

$$\Omega'_\Lambda = -2\Omega_\Lambda \left(\frac{\dot{H}}{H^2} + \frac{\sqrt{\Omega_\Lambda}}{na} \right). \tag{41}$$

Taking the derivative of the BI equation (3) with respect to the cosmic time, and using Eqs. (8), (10), (35) and (37), it is easy to find

$$\frac{\dot{H}}{H^2} = -\frac{3}{2}\left(1 - b^2 - \frac{\Omega_\Lambda}{1-\Omega_{\sigma 0}} + \frac{2}{3na}\frac{\Omega_\Lambda^{\frac{3}{2}}}{1-\Omega_{\sigma 0}}\right). \tag{42}$$

Combining Eqs. (41) and (42), we have the equation of motion, a differential equation, for Ω_Λ

$$\Omega'_\Lambda = 3\Omega_\Lambda \left(1 - b^2 - \frac{\Omega_\Lambda}{1-\Omega_{\sigma 0}} - (1 - \frac{\Omega_\Lambda}{1-\Omega_{\sigma 0}})\frac{2\sqrt{\Omega_\Lambda}}{3na}\right). \tag{43}$$

As shown in Ref. [18], the parameters n and Ω_{mo} are not independent of each other. If one takes them as free parameters, the NADE model will become confused. Therefore the initial conditions in NADE should be taken at the early times. Alike Ref. [18] proposed the initial condition for the case of ADE, $\Omega_\Lambda = n^2 a^2/4$, at $z = 1/a - 1 = 2000$, so Eq. (43) can be numerically solved. In Fig. (2) we have depicted the evolution of Ω_Λ as a function of scale factor for various values of the free parameters for this model. In the left part of this figure show the effects of the anisotropic on the evolutionary behaviour the NADE model. In the middle and right panel of Fig. (2), evolution of Ω_Λ is plotted for different choices of b^2 and n. These figures shows that for larger (smaller) values of b^2 (n) the evolution of Ω_Λ will be flatter. Also, figures illustrates the Ω_Λ increase with the a increase but:I) increase of the $\Omega_{\sigma 0}$ cause the Ω_Λ increases with sharper slope. II) Increasing the coefficient coupling cause the early and final Ω_Λ values to ($a << (>>)$) increases (decreases) respectively III) at last, increase of n parameter cause the Ω_Λ parameter pick smaller value for the smaller scale factor i.e. $a <<$.

A. Quintessence reconstruction of NADE in BI

Now we suggest a correspondence between the new agegraphic dark energy and quintessence scalar field namely, we identify ρ_ϕ to be ρ_Λ. Using relation $\rho_\phi = \rho_\Lambda = 3M_p^2 H^2 \Omega_\Lambda$ and substituting Eqs. (37) and (39) into (17) and (18)

one can readily find the kinetic energy term and the potential term as

$$\dot{\phi}^2 = M_p^2 H^2 \left(\frac{2}{na} \Omega_\Lambda^{\frac{3}{2}} - 3b^2(1-\Omega_{\sigma 0}) \right), \tag{44}$$

$$V(\phi) = M_p^2 H^2 \left(3\Omega_\Lambda + \frac{3b^2}{2}(1-\Omega_{\sigma 0}) - \frac{\Omega_\Lambda^{\frac{3}{2}}}{na} \right). \tag{45}$$

From definition $\dot{\phi} = H\phi'$, one can rewrite Eq. (44) as

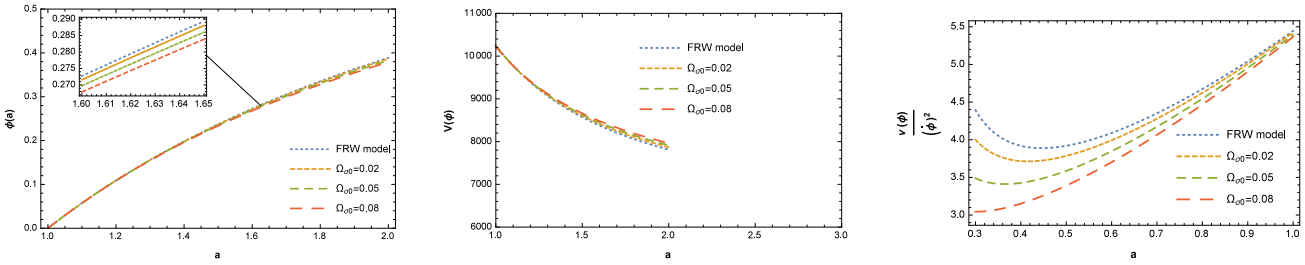

FIG. 3: Left panel: The plot shows the evolution of the NADE quintessence scalar filed, Eq. (46), for four different value of the anisotropy energy density parameter $\Omega_{\sigma 0}$. Middle panel: The plot shows the NADE quintessence potential, Eq. (45), versus the scale factor for different $\Omega_{\sigma 0}$. Right panel: The plot shows the NADE quintessence $\frac{V(\phi)}{\dot{\phi}^2}$, for different value of $\Omega_{\sigma 0}$. Auxiliary parameters are $\Omega_\Lambda^0 = 0.72$, $b^2 = 0.02$, $n = 2.886$ and $\phi(1)$=0.

$$\phi' = M_p \left(\frac{2}{na} \Omega_\Lambda^{\frac{3}{2}} - 3b^2(1-\Omega_{\sigma 0}) \right)^{\frac{1}{2}}. \tag{46}$$

Therefore, we have established an interacting new agegraphic quintessence dark energy model and reconstructed the potential of the agegraphic quintessence as well as the dynamics of scalar field in an anisotropic universe. Basically, from Eqs. (43) and (46) one can derive $\phi = \phi(a)$ and then combining the result with (45) one finds $V = V(\phi)$. Unfortunately, the analytical form of the potential in terms of the new agegraphic quintessence field cannot be determined due to the complexity of the equations involved. However, we can obtain it numerically. The evolution of the NADE quintessence scalar filed, Eq. (46), for four different values of $\Omega_{\sigma 0}$ is plotted in left Fig. 3. We see that the differences in the shapes of ϕ are very little. Figure 3 shows that the scalar field increases (and hence the kinetic energy $\dot{\phi}^2$ of the potential decreases) with the passage of time. The potential $V(\phi)$ versus a for four different value of the $\Omega_{\sigma 0}$ are shown in middle panel of Fig. (3), indicating the decreasing behavior. It illustrate for a given $\Omega_{\sigma 0}$, $V(\phi)$ decreases with increasing a and the curve is shifted to the smaller values of $V(\phi)$ with decreasing the $\Omega_{\sigma 0}$. Also, we see from these figures that the cosmic evolution trends are quite similar for these four anisotropy energy density parameters. The evolution of $V(\phi)/\dot{\phi}^2$ versus a is illustrated in right Fig. (3). It illustrate fraction of potential per kinetic energy increase with the a increase and its magnitude increase with the $\Omega_{\sigma 0}$ decrease for the smaller a.

B. Tachyon reconstruction of NADE in BI

Next, we reconstruct the new agegraphic tachyon DE model, connecting the tachyon scalar field with the NADE in BI universe. Using Eqs. (37) and (39) one can easily show that the tachyon potential and kinetic energy term take the following form

$$V(\phi) = 3M_p^2 H^2 \Omega_\Lambda \left(1 - \frac{2}{3na}\sqrt{\Omega_\Lambda} + \frac{b^2}{\Omega_\Lambda}(1-\Omega_{\sigma 0}) \right)^{\frac{1}{2}}, \tag{47}$$

$$\dot{\phi} = \left(\frac{2}{3na}\sqrt{\Omega_\Lambda} - \frac{b^2}{\Omega_\Lambda}(1-\Omega_{\sigma 0}) \right)^{\frac{1}{2}}. \tag{48}$$

Therefore the evolution behavior of the tachyon field can be obtained by integrating the above equation

$$\phi(a) - \phi(1) = \int_1^a \frac{1}{Ha} \sqrt{\frac{2}{3na}\sqrt{\Omega_\Lambda} - \frac{b^2}{\Omega_\Lambda}(1-\Omega_{\sigma 0})}\, da, \tag{49}$$

where Ω_Λ is given by Eq. (43). The evolutionary form of the tachyon field and the reconstructed tachyon potential

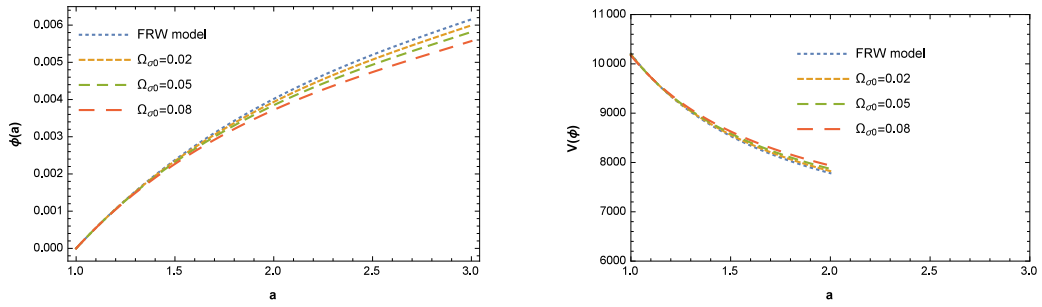

FIG. 4: Right panel: The evolution of the NADE tachyon scalar filed, Eq. (49), for different the anisotropy energy density parameter $\Omega_{\sigma 0}$. Right panel: The NADE tachyon potential, Eq. (47), versus the scale factor for different $\Omega_{\sigma 0}$. Auxiliary parameters as in Fig. (3).

$V(\phi)$ are plotted in Fig. (4), where again we have taken $\phi(a_0 = 1) = 0$ for the present time. Selected curves are plotted for different value of the anisotropy density parameter $\Omega_{\sigma 0}$. From this figure we find out that ϕ increases with time while the potential $V(\phi)$ becomes steeper with decreasing $\Omega_{\sigma 0}$. This behavior is in agreement with the scaling solution $V(\phi) \propto \phi^{-2}$ obtained for the tachyon filed corresponding to the power law expansion [43]. As the isotropic ($\Omega_{\sigma 0} = 0$) case the scalar field has a non-zero minimum, which leads to an EoS parameter close to -1 for present time and near future. Again from right panel of Fig. (4) we find out the reconstructed scalar field has a same potential as the quintessence case.

C. K-essence reconstruction of NADE in BI

The K-essence scalar field model is also an interesting attempt to explain the origin of DE using string theory. Equating ω_K with the EoS parameter of NADE (39) one finds

$$\chi = \frac{2 - \frac{2}{3na}\sqrt{\Omega_\Lambda} + \frac{b^2}{\Omega_\Lambda}(1 - \Omega_{\sigma 0})}{4 - \frac{2}{na}\sqrt{\Omega_\Lambda} + \frac{3b^2}{\Omega_\Lambda}(1 - \Omega_{\sigma 0})}. \tag{50}$$

Using Eq. (50) and $\dot{\phi}^2 = 2\chi$, we obtain the new agegraphic K-essence scalar field as

$$\phi(a) - \phi(1) = \int_1^a \frac{1}{Ha}\sqrt{\left(\frac{4 - \frac{4}{3na}\sqrt{\Omega_\Lambda} + \frac{2b^2}{\Omega_\Lambda}(1 - \Omega_{\sigma 0})}{4 - \frac{2}{na}\sqrt{\Omega_\Lambda} + \frac{3b^2}{\Omega_\Lambda}(1 - \Omega_{\sigma 0})}\right)}da. \tag{51}$$

where we take $a_0 = 1$ for the present time. The evolution of the field and the reconstructed K-essence kinetic energy $\chi(\phi)$ are plotted in Fig. (5), where we have taken $\phi(a_0 = 1) = 0$ for simplicity. Note that in left Fig. (5) the field

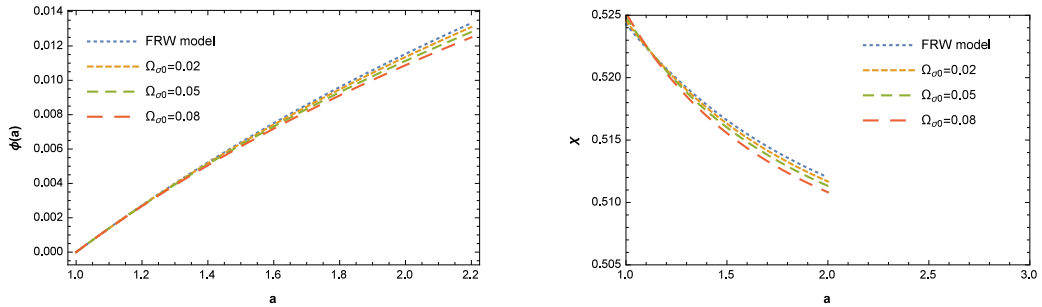

FIG. 5: Right panel: The K-essence scalar field as function of the scale factor for the values of the $\Omega_{\sigma 0}$. Left panel: The evolution of the new agegraphic K-essence kinetic energy $\chi = \dot{\phi}^2/2$ for different constant anisotropy $\Omega_{\sigma 0}$. Auxiliary parameters as in Fig. (3).

increases with the increment of a. Obviously, the kinetic energy decreases with increasing the scale factor as shown in right panel of Fig. (5). Figure 5 shows that $\chi(\phi)$ almost lies in the required interval $(0.505, 0.525)$ from early epoch to the later time. The EoS parameter ω_K indicates that the accelerated universe can be obtained for this interval.

V. COSMOLOGICAL EVOLUTION OF THE INTERACTING HDE AND NADE MODEL IN BI MODEL

In order to fit the model with current observational data, we consider the interacting NADE model in a flat BI universe in this section. In this case, the Hubble parameter can be written as,

$$H = H_0\sqrt{\frac{\Omega_m(1+z)^3 + (1-\Omega_m-\Omega_{\sigma 0})X(z)}{1-\Omega_{\sigma 0}}}, \tag{52}$$

where $X(z) = \rho_\Lambda(z)/\rho_{\Lambda 0}(z)$. For the case of FRW ($\Omega_{\sigma 0} = 0$) which are in agreement with the respective relations obtained in [50]. Here Ω_{m0} is present value of dimensionless energy density of matter and z is the redshift, $z = 1/a - 1$. Note that, for simplicity, in this work we disregard the contributions from baryons and radiation. For the ΛCDM model, $H(z)$ as $H = H_0\sqrt{\Omega_{m0}(1+z)^3 + \Omega_\Lambda}$. Also, for model such as wCDM (with the constant EoS w), it is $H = H_0\sqrt{\Omega_{m0}(1+z)^3 + (1-\Omega_{m0}-\Omega_{\sigma 0})(1+z)^{3(1+w)}}$. The currently preferred values of w in this model is $w = -1.01 \pm 0.15$ [49]. To constrain cosmological parameters we use the $H(z)$ data from SVJ [52], DA method [53], Jimenez [54] and Clustering [55]. These data, for the redshift range $0 < z < 2$, are shown in figure 6, and we find a remarkable agreement between the different measurements. The value of $H(z)$ is then directly computed by using Eq. (3). In top panel of Fig. (6), we show four models, namely, NADE, HDE, ΛCDM and wCDM models. We see from this figure that the cosmic evolution trends are quite similar for three models, such as, NADE, ΛCDM and wCDM models. So, among these four DE models, HDE with the Hubble radius H^{-1} in BI is not favored by the observational data. Also from middle panel of Fig. (6), we can clearly see that for different values of $\Omega_{\sigma 0}$ the process of cosmic evolution looks quite similar, i.e., for the bigger value the parameter $\Omega_{\sigma 0}$ is taken, the bigger value the Hubble expansion rate $H(z)$ is gotten. For this model, we consider, $H_0 = 72\ kms^{-1}Mpc^{-1}$, as the value of $H_0 = 73 \pm 3\ kms^{-1}Mpc^{-1}$ from the combination WMAP 3 year estimate [57], and the other with $H_0 = 68 \pm 4\ kms^{-1}Mpc^{-1}$ from a median statistics analysis of 461 [58]. The evolution of the σ is plotted in left panel of Fig. (7). From Fig. (7), it can be observed that evolution of shear depends on the initial conditions. Signature change of shear can be seen for certain kind of DE. Also, the shear scalar becomes negligible at late times and σ of NADE decreases slowly for walls compared to the HDE. Finally we have considered, the model isotropize. The measure of the anisotropy is described by σ/H, describe the magnitude of the spacetime shear per the average expansion rate. However, as shown in right panel of Fig. (7), during the inflationary phase, we find that the effect of shear cannot become as large as the Hubble parameter and the shear decreases at the end of the inflation.
In the following, we constrain the model parameters of these DE models in BI universe by using the $H(z)$ measurements.

A. SL test

The redshift-drift observation, sometimes called the "SL test", is not only conceptually simple, but also is a direct probe of cosmic dynamic expansion, although being observationally challenging. Ref. [50] introduced the redshift relation by the a spectroscopic velocity shift $\Delta\nu$ as $\Delta\nu \equiv \Delta z/(1+z)$. By using the Hubble parameter $H(z) = -\dot{z}/(1+z)$ and Eq. (3), we obtain

$$\Delta\nu = H_0\Delta t_0\left(1 - \frac{E(z)}{1+z}\right), \tag{53}$$

where we set $\Delta t_0 = 10$ years, and $E(z) = H(z)/H_0$. According to the Monte Carlo simulations, the uncertainty of $\Delta\nu$ measurements expected by CODEX can be expressed as [59]

$$\sigma'_{\Delta\nu} = 1.35(\frac{2370}{S/N})\sqrt{\frac{30}{N_{QSO}}}(\frac{5}{1+z_{QSO}})^{1.8}cm/s, \tag{54}$$

where $S/N = 3000$ is the signal-to-noise ratio, $N_{QSO} = 30$ is the number of observed quasars and $z_{QSO} \in [2, 5]$ is their redshift. We will examine the Sandage-Loeb (SL) test, and then examine effects of anisotropy and parameter

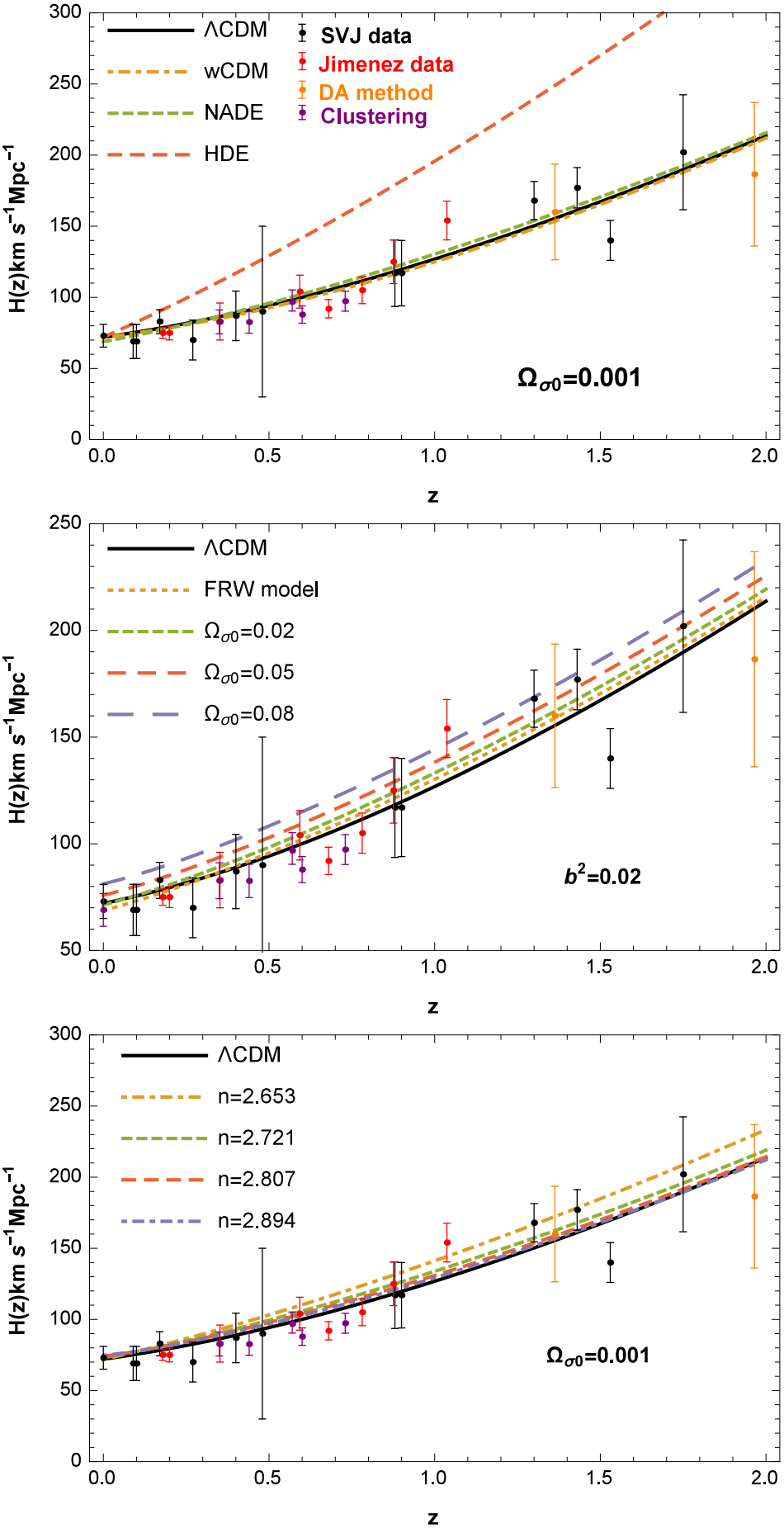

FIG. 6: Upper panel: Comparison of the observed $H(z)$, with the predictions from the NADE, HDE, ΛCDM and wCDM models. Middle panel the evolution of $H(z)$ versus redshift z in NADE anisotropic universe for different values of parameter $\Omega_{\sigma 0}$ with $n = 2.886$ and the ΛCDM models while bottom panel the evolution of $H(z)$ versus redshift z for different values of

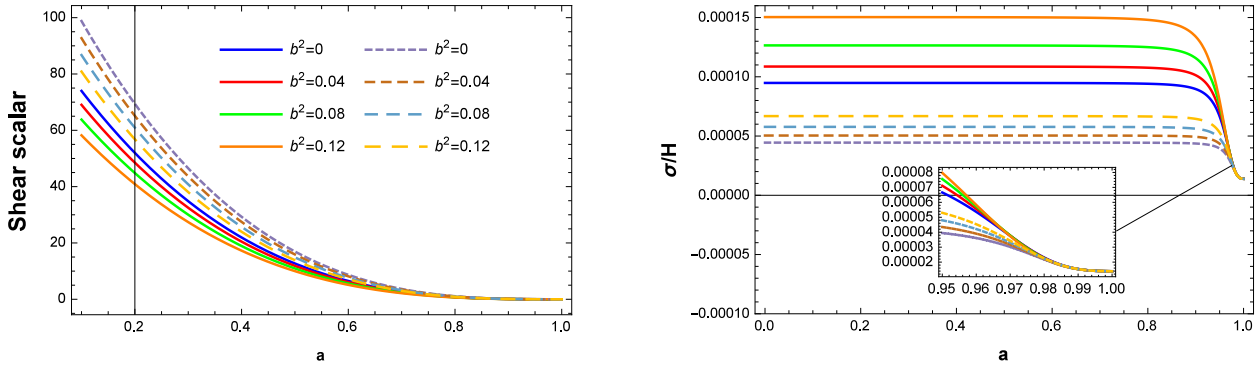

FIG. 7: Left panel: Time evolution of the shear scalar for different value of b^2 and $\sigma_0 = 0.05$ [56]. Right panel: The evolution of the anisotropy parameter σ/H with respect to the scale factor a in a BI universe. It becomes almost constant during the anisotropic inflationary phase. Then it falls rapidly down to $\mathcal{O}(\sigma\mathcal{H})$. As shown in the legend, the interacting NADE is shown with the thin lines, and the interacting HDE with the dashed lines. The initial data is same as in Fig. (6).

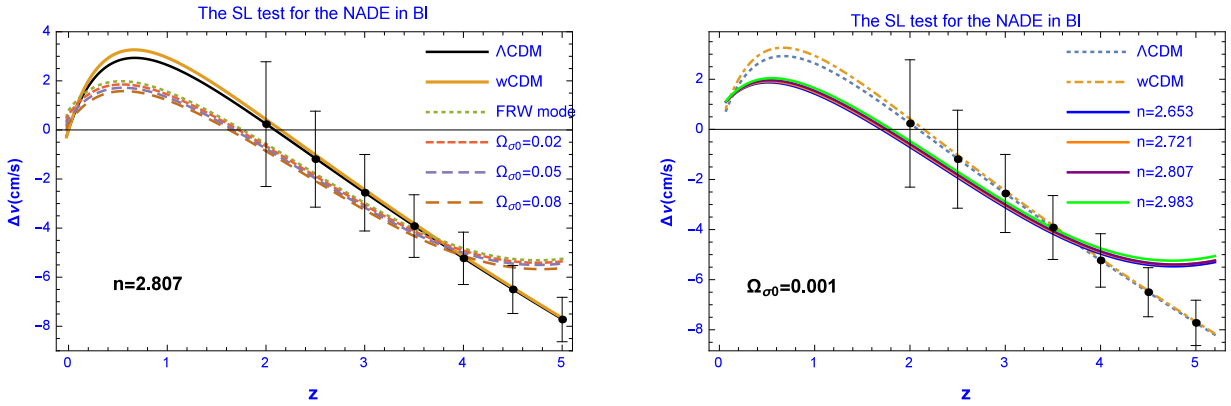

FIG. 8: Cosmic velocity shift as function of the redshift for the NADE model with four different values of $\Omega_{\sigma 0}$ (left panel) and n (right panel), the ΛCDM model with $\Omega_\Lambda^0 = 0.7$ and wCDM model with $w = -1.07$ and $\Omega_{m0} = 0.3$. A time interval of 10 years has been assumed. The data points and error bars are estimated from Eq. (54) with a fiducial concordance ΛCDM model.

of n on the NADE in the SL test as shown in Fig. (8). We have chosen the fractional matter density $\Omega_{m0} = 0.274$ from ΛCDM [25] and $n = 2.807$ [47]. In left panel of Fig. (8), the parameter n is fixed to be 2.807 for the NADE model, and the parameter $\Omega_{\sigma 0}$ of the NADE model is variable while in right panel, we fix $\Omega_{\sigma 0} = 0.001$ and vary n for the NADE model in BI universe. Based on the parameter spaces constrained from the current data combination, the boundaries of $\Delta\nu$ could be determined by using Eq. (53). We also plot the error bars in the SL test, given by Eq. (54), on the corresponding bands, in order to make a direct comparison with the reconstructed results from the current data. From Fig. (8) we see that the NADE in BI model can be distinguished from the ΛCDM and wCDM models via the SL test. As we can observe $\Delta\nu$ is positive at small redshifts and becomes negative at $z \geq 1.7$. This result is reasonable with Refs. [50, 51, 60]. Beside, the amplitude and slope of the signal depend mainly on both $\Omega_{\sigma 0}$ and n.

B. The statefinder diagnostic

Since there are so many DE models that have been put forward, in order to discriminate different DE models from each other, Sahni *et al.* [61] introduced the statefinder pair $\{r, s\}$, which uses the third time derivative of the scale factor $a(t)$, to diagnose and discriminate behaviors of different DE models. In the following, we consider the statefinder parameters $\{r, s\}$ [61–64] for the present case. The r, s parameters are given by [61]

$$r \equiv \frac{\dddot{a}}{aH^3}, \qquad s \equiv \frac{r-1}{3(q-\frac{1}{2})}. \tag{55}$$

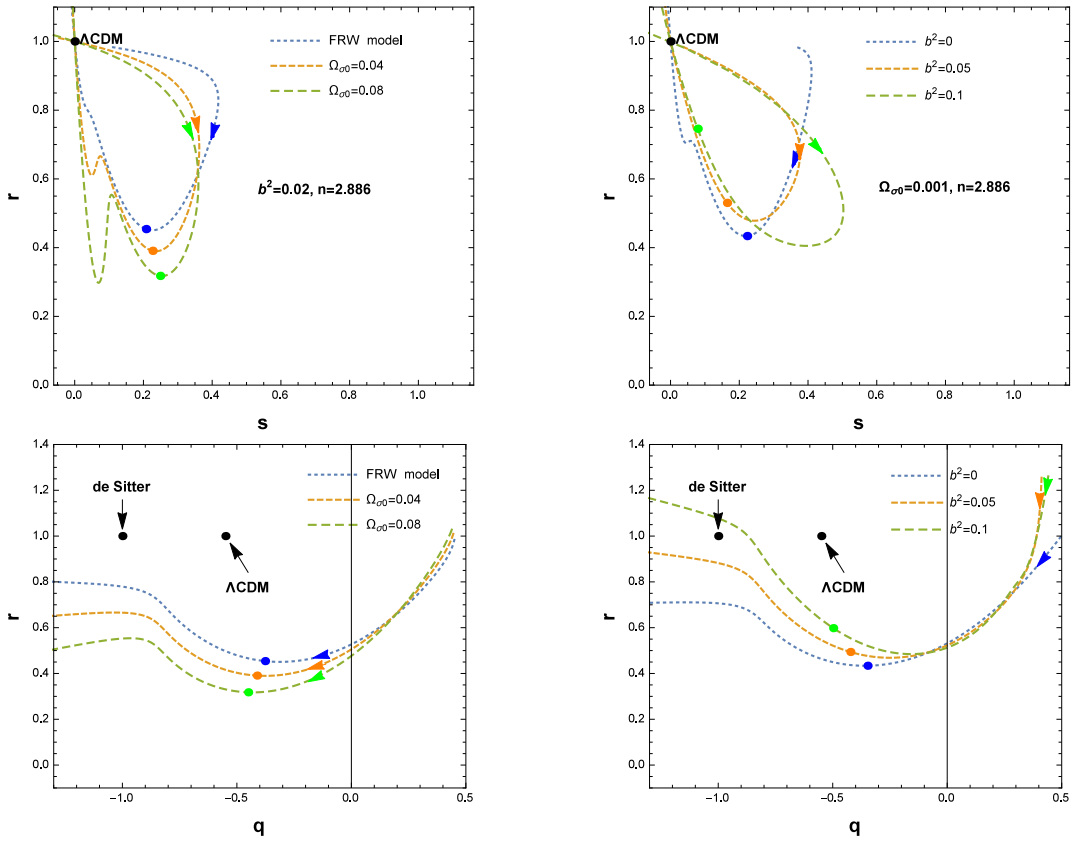

FIG. 9: Top panel: The statefinder diagrams $r(s)$ for the interacting NADE in BI model. The ΛCDM model corresponds to a fixed point $\{0,1\}$. The dots show today's values for the statefinder parameters (s_0, r_0). Bottom panel: Evolutionary trajectory in the $r-q$ plane for interacting NADE model in BI universe.

We will soon see that it has a remarkable property for the basic flat ΛCDM BI model. The statefinder parameter s is a linear combination of r and q. In the $\{r,s\}$ plane, $s>0$ corresponds to a quintessence-like model of DE and $s<0$ corresponds to a phantom-like model of DE. Then, by using the BI equation, we can obtain the following concrete expressions

$$r = 1+\frac{3}{2}\Omega_{\sigma 0}+\frac{9}{2}\frac{\Omega_\Lambda\omega_\Lambda}{1-\Omega_{\sigma 0}}(1+\omega_\Lambda+\Omega_{\sigma 0})+\frac{9}{2}\omega_\Lambda b^2-\frac{3}{2}\frac{\Omega_\Lambda\omega'_\Lambda}{1-\Omega_{\sigma 0}},$$
$$s = \frac{\Omega_{\sigma 0}+\frac{3\Omega_\Lambda\omega_\Lambda}{1-\Omega_{\sigma 0}}(1+\omega_\Lambda+\Omega_{\sigma 0})+3\omega_\Lambda b^2-\frac{\Omega_\Lambda\omega'_\Lambda}{1-\Omega_{\sigma 0}}}{3\omega_\Lambda\Omega_\Lambda-\Omega_{\sigma 0}}, \tag{56}$$

where Ω_Λ is given by (43) and $\omega'_\Lambda=\left(\frac{\sqrt{\Omega_\Lambda}}{na}+\frac{3b^2(1-\Omega_{\sigma 0})}{\Omega_\Lambda}\right)\left(1-b^2-\frac{\Omega_\Lambda}{1-\Omega_{\sigma 0}}-\frac{2}{3na}(1-\frac{\Omega_\Lambda}{1-\Omega_{\sigma 0}})\sqrt{\Omega_\Lambda}\right)$. So by solving Eq. (43) we can get the evolution solution of Ω_Λ and then hold all the cosmological quantities of interest and the whole dynamics of the universe. The $\{r,s\}$ evolutionary trajectory in the interacting NADE model for different values of $\Omega_{\sigma 0}$ and b^2 are shown in top panel of Fig. 9. The arrows in the diagram denote the evolution directions of the statefinder trajectories and the color dots show present-day values for the statefinder parameters. The crossing with ΛCDM occurs for this case. In the statefinder $\{r,s\}$ plane, the ΛCDM model in the flat universe corresponds to a fixed point $\{r,s\}=\{1,0\}$, and the other models of DE's behaviors can be measured from the distance between them and the ΛCDM point. From Fig. 9, we can find that the the larger anisotropy parameter makes the value of r smaller and the value of s bigger while the the larger interaction between dark components makes the value of s smaller and the value of r bigger, evidently. From this figure one can observe that, in the low-redshift region, the difference between the NADE models and the ΛCDM model can be easily distinguished, which is quite different from the cases of $H(z)$ (see Fig. 6). As a complementarity, bottom panel of Fig. 9 shows another statefinder diagram $r-q$ evolutionary trajectory. In the statefinder $r-q$ plane, the de Sitter model in the flat universe corresponds to a fixed point $(r=1,q=-1)$. According to the interacting NADE model, for the limiting case $b^2=0.02$, the current

universe corresponds to a point $(r_0 = 0.454, s_0 = 0.207, q_0 = -0.377)$, $(r_0 = 0.391, s_0 = 0.226, q_0 = -0.412)$ and $(r_0 = 0.317, s_0 = 0.248, q_0 = -0.451)$ when $\Omega_{\sigma 0} = 0, 0.04, 0.08$, respectively while for the limiting case $\Omega_{\sigma 0} = 0.001$, we have $(r_0 = 0.433, s_0 = 0.222, q_0 = -0.348)$, $(r_0 = 0.530, s_0 = 0.164, q_0 = -0.423)$ and $(r_0 = 0.745, s_0 = 0.079, q_0 = -0.498)$ when $b^2 = 0, 0.05, 0.1$, respectively.

C. Linear perturbation theory

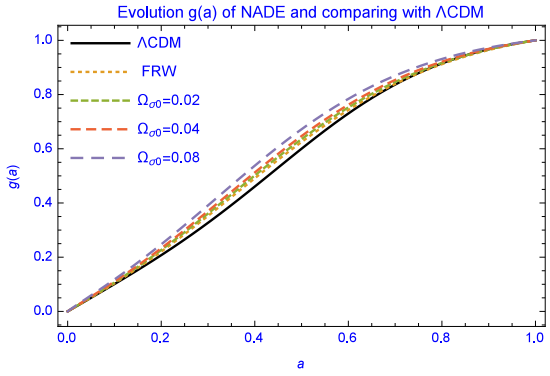

FIG. 10: Time evolution of the growth factor for different value of the anisotropy energy density parameter $\Omega_{\sigma 0}$ and comparing to the ΛCDM and FRW in NADE models with $n = 2.807$.

In this subsection, we study the linear growth of perturbation of non relativistic dust matter by computing the evolution of growth factor $g(a)$ in NADE model, and then compare it with the evolution of growth factor in NADE of FRW and ΛCDM models. In this case the differential equation for the evolution of $g(a)$ is given by [65, 66]

$$g''(a) + \left(\frac{3}{a} + \frac{E'(a)}{E(a)}\right) g'(a) - \frac{3}{2}\frac{\Omega_{m0}}{a^5 E^2(a)} g(a) = 0. \tag{57}$$

In order to study the linear growth in NADE model, using Eqs. (39), (43) and (52) for BI universe, we solve numerically Eq. (57). In addition, we solve numerically (57) for the FRW model and the ΛCDM model. To evaluate the initial conditions, since we are in the linear regime, we assume that the linear growth factor has a power law solution, $g(a) \propto a^m$ [65], with m, to be evaluated at the initial time. We plot the evolution of $g(a)$ with respect to a function of the scale factor in Fig. (10). In the ΛCDM model, the growth factor evolves more slowly compared to the NADE in FRW universe because the expansion of the universe slows down the structure formation. Also, in the NADE of FRW model, the growth factor evolves more slowly compared to the NADE in BI model. This behavior can be explained by taking into account the evolution of Hubble parameter in Fig. (6). Therefore the growth factor $g(a)$ for the ΛCDM and DE of FRW model will always fall behind the NADE in anisotropic universe.

D. Distance modulus

Finally, we consider constraints on model parameters coming from SNIa observations. Observation of SNIa does not provide standard ruler but rather gives distance modulus. This quantity is defined by [67]

$$\mu_{th}(z) = 5 \log_{10} \frac{D_L(z)}{Mpc} + 25. \tag{58}$$

The luminosity distance $D_L(z)$ is given by

$$D_L(z) = (1 + z) r(z), \tag{59}$$

where $r(z) = \int_0^z H^{-1}(z')dz'$. In all, current SNIa data are unable to discriminate between the popular ΛCDM and our interaction model. In Fig. 11, we show the dimensional marginalized contour in the $c - \Omega_{\sigma 0}$ for the HDE model in an anisotropic universe. The fit values for the model parameters is $c = 0.994^{+0.126}_{-0.065}$ at the moment time i.e. $z \to 0$. As is clear from figure 11 the parameter c increases with the decreasing anisotropy parameter and this is consistent

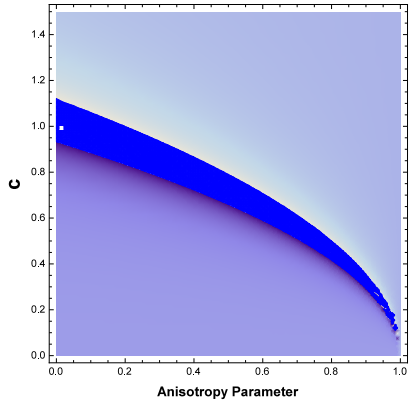

FIG. 11: The constraints on the HDE model in the $c - \Omega_{\sigma 0}$ plane from the current $H(z)$ measurements in an anisotropic universe.

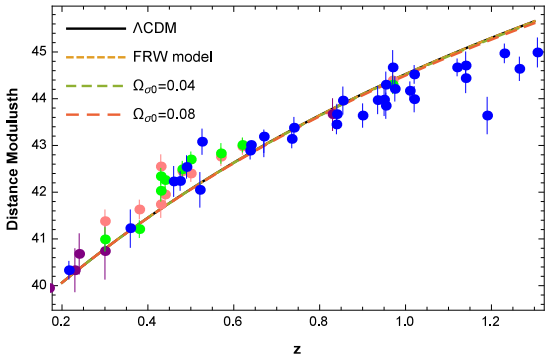

FIG. 12: Distance modulus for the best fit model $\Omega_{m0} = 0.288$, $H_0 = 72\ km/s/Mpc$, $b^2 = 0.02$, $n = 2.807$ and the ΛCDM model, $\Omega_{m0} = 0.3$, $H_0 = 72\ km/s/Mpc$ and $\Omega^0_\Lambda = 0.7$. The data points are from the gold and Silver SNe Ia of [68, 69].

with the observed data. We can also measure $D_L(z)$ through the Hubble parameter by using the Eqs. (20) and (52). Figure 12 presents the distance modulus with the best fit of our model and the best fit of the ΛCDM model to the Gold and Silver SNe Ia data sets of [68, 69]. We add 4 SNe Ia from this current paper. From Fig. 12 we can observe the universe is accelerating expansion. In all, current data are unable to discriminate between the popular ΛCDM, FRW and our interaction models as shown in Fig. (12).

VI. CONCLUSION AND DISCUSSION

In this work, we have investigated the different models of cosmology in an anisotropic universe, when we are using the scalar field models. In particular, we reconstructed the field equations of DE model in an anisotropic universe. Then we have reconstructed both the potentials and the kinetic energies corresponding to each model, which describe quintessence, tachyon and K-essence cosmology. In addition, we have discussed main features by choosing different values of interacting parameter b^2 and different value of the anisotropy energy density parameter $\Omega_{\sigma 0}$, which are summarized as follows.

- The simplest choice is the Hubble scale $L = 1/H$, giving a energy density that is comparable to the present-day DE [5, 39]. It has been argued that an IR cutoff defined by the Hubble radius, the DE results as pressureless so can not lead to an accelerated universe. We have also shown that taking into account the interaction [35, 38] and anisotropy terms, we are able to describe the accelerating universe. In the following, by using the Hubble radius as $L = H^{-1}$ IR cutoff, combinations of the HDE model and interacting scalar fields in anisotropic universe were implemented. We have obtained expressions for the scalar field and the potential for interacting HDE in BI model. The free parameters of cosmology have been evaluated in terms of the constants b^2, $\Omega_{\sigma 0}$ and c^2. The results of our analysis are displayed in Fig. (11). We used current observational data to constrain the HDE model. The fit values for the model parameters is $c = 0.994^{+0.126}_{-0.065}$ at the moment time.

- The EoS parameter ω_Λ of the NADE model in the BI models, can cross the phantom divide line ($\omega_\Lambda < -1$) at the present time, provided that $b^2 \geq 0.08$ which is compatible with the observations. By the way, the effect of various $\Omega_{\sigma 0}$ were negligible but as $a \to 0$, it was clear that decreasing of the $\Omega_{\sigma 0}$ cause to decrease the EoS parameter as shown in left panel of figure 1. This type of behavior is consistent with the present observations. In the Fig. (2) it have been illustrated, the Ω_Λ increased with the a increase but:I) increase of the $\Omega_{\sigma 0}$ caused the Ω_Λ increases with sharper slope. II) Increasing the coefficient coupling caused the early and final Ω_Λ value to increased III) at last, increase of n parameter caused the Ω_Λ parameter picked smaller value for the smaller scale factor i.e. $a <<$.

- The new agegraphic quintessence scalar filed for a given $\Omega_{\sigma 0}$, increases with increasing the scale factor, also, the curve was shifted to the larger value of ϕ with decreasing $\Omega_{\sigma 0}$ as shown in left panel of Fig. (3). For a given $\Omega_{\sigma 0}$, potential $V(\phi)$ decrease with increasing the scale factor and the curve is shifted to the bigger values of $V(\phi)$ with increasing the $\Omega_{\sigma 0}$ as shown in figure 3 (middle panel). Right panel of Fig. (3) shown which the fraction of potential per kinetic energy increase with the a increase and its magnitude increase with the $\Omega_{\sigma 0}$ decrease for the smaller a.

- The new agegraphic tachyon scalar filed for a given $\Omega_{\sigma 0}$ behave like the new agegraphic quintessence model as shown in figure 4.

- We have evaluated the interacting NADE versions of K-essence scalar field in BI models. These results have been shown in Fig. (5). The new agegraphic K-essence scalar field for a given $\Omega_{\sigma 0}$ increases with increasing the scale factor. But its kinetic energy decreases. For a given scale factor, the new agegraphic K-essence scalar filed and kinetic energy decreases with increasing $\Omega_{\sigma 0}$. Anyway, we have shown that the evolution of the NADE scalar filed and kinetic energy in anisotropic universe is smaller than the evolution of the NADE scalar filed and kinetic energy in FRW space time. But its potential large.

- Considering a BI model and interacting between DE and DM we have reconstructed Hubble parameter $H(z)$ (see Fig. (6)) versus the redshift z and it compared the observed expansion rate $H(z)$ with that predicted by the four DE models. We have used the SVJ, DA method and Jimenez Hubble parameter versus redshift data to constrain cosmological parameters of different DE models. The constraints are restrictive, and consistent with those determined by using type Ia supernova redshift-magnitude data. The reconstructed Hubble parameter is found to be decreasing with evolution of the universe and according to this model, the evolution of the accelerated expansion of the universe is speedy than the evolution of the isotropic model. It is seen that among different DE models, only the curve of $H(z)$ predicted by the NADE model. So, HDE with the Hubble radius $1/H$ in BI is not favored by the observational data. We analyzed the evolution of the shear scalar in right panel of Fig. (7), which is depending on the initial conditions and we found that there can be a sign change in the shear. This may have some interesting implications in early universe cosmology. Furthermore, we have studied the evolution of the σ/H as shown in left panel of figure 7. Although the shear is constant during the inflation, it can fall at the end of the inflation. Moreover, we have seen that the anisotropy of the universe σ/H can increase to $\mathcal{O}(1)$ at the end of the inflation. In the following, we showed that the SL test data are extremely helpful in breaking the existing parameter degeneracies. We analyzed how the SL test would impact on the DE constraints from the future geometric measurements. Therefore, the SL test can be used to distinguish the NADE of FRW and NADE of BI models from the ΛCDM, the wCDM and it was observed that the constraint on $\Omega_{\sigma 0}$ and n are very strong (see Figs. (8)). Comparing the dynamical behaviour of the expansion expected in anisotropic universe with isotropic universe. We apply the statefinder diagnostic to the NADE model with interaction in BI models. The statefinder diagrams show that the interaction between DE and DM can significantly affect the evolution of the universe and the contributions of the interaction can be diagnosed out explicitly in this method. We plot the evolutionary trajectories of this model in the statefinder parameter planes as shown in Fig. (9). The statefinder diagnostic can be performed to the NADE model in cases of different $\Omega_{\sigma 0}$ and b^2, which indicates that the values of $\Omega_{\sigma 0}$ and b^2 determines the evolution behavior and the fate of the universe. The BI NADE model can reach the ΛCDM point $\{1, 0\}$ in the $r - s$ plane. In the limiting case of $b^2 = 0.02$, the trajectories of $r - s$ plane with all values of $\Omega_{\sigma 0}$ approaches to quintessence behavior as well as corresponds to ΛCDM limit as shown in top panel of Fig. (9). It is also valid for $\Omega_{\sigma 0} = 0.001$ with different values of b^2. In addition, the $r - q$ plane has been used for discussion on the evolutionary property of the BI universe (see bottom panel of Fig. (9)). We have also studied the effects of anisotropy on the growth of structures in linear regime for the current model. Referring to Fig. (10) it is observed that the growth factor $g(a)$ for the ΛCDM and DE of FRW model will always fall behind the NADE in an anisotropic universe. In addition to this we discuss the distance modulus with the best fit of our model and the best fit of the ΛCDM model to the Gold and Silver SNe Ia data sets of [68, 69]. In Fig. (12) we are able to discriminate between the ΛCDM, FRW and NADE in BI model.
  Finally, we would like to mention that the aforementioned discussion in first part this work can be easily

generalized to other choices of IR cut-off, namely, Ricci length scale and radius of the event horizon (for this point see also, e.g., [70]).

---

[1] A.G. Riess, A.V. Filippenko, P. Challis *et al.*, Astron. J. **116**, 1009 (1998).
[2] S. Perlmutter, G. Aldering, G. Goldhaber, *et al.*, Astrophys. J. **517**, 565 (1999).
[3] L. Susskind, J. Math. Phys. **36**, 6377 (1995).
[4] G.'t Hooft, Int. J. Mod. Phys. D **15**, 1587 (2006).
[5] S.D. Thomas, Phys. Rev. Lett. **89**, 081301 (2002).
[6] M. Gasperini *et al.*, Phys. Rev. D **65**, 023508 (2002).
[7] M. Li, Phys. Lett. B **603**, 1 (2004).
[8] A.G. Cohen, D.B. Kaplan, A.E. Nelson, Phys. Rev. Lett. **82**, 4971 (1999).
[9] R.C. Myers, M.J. Perry, Annals Phys. **172**, 304 (1986).
[10] B. Wang, Y. Gong and E. Abdalla, Phys. Lett. B **624**, 141 (2005).
[11] Anjan A. Sen, D. Pavón, Phys. Lett. B **664**, 7 (2008).
[12] S.D.H. Hsu, Phys. Lett. B **594**, 13 (2004).
[13] D. Pavón and W. Zimdahl, Phys. Lett. B **628**, 206 (2005).
[14] E.N. Saridakis, Phys. Lett. B **660**, 138 (2008).
[15] J. Zhang, X. Zhang and H. Liu, Eur. Phys. J. C **52**, 693 (2007).
[16] R.G. Cai, Phys. Lett. B **657**, 228 (2007).
[17] H. Wei, R.G. Cai, Eur. Phys. J. C **59**, 99 (2009).
[18] H. Wei and R.G. Cai, Phys. Lett. B **660**, 113 (2008).
[19] H. Wei and R.G. Cai, Phys. Lett. B **663**, 1 (2008).
[20] J.-P. Wu, D.-Z. Ma and Y. Ling, Phys. Lett. B **663**, 152 (2008).
[21] I.P. Neupane, Phys. Lett. B **673**, 111 (2009).
[22] K. Karami, S. Ghaffari, J. Fehri, Eur. Phys. J. C **64**, 85 (2009).
[23] J. Zhang, X. Zhang, H. Liu, Eur. Phys. J. C **54**, 303 (2008).
[24] Y.H Li, J.Z. Ma, J.L. Cui, Z. Wang and X. Zhang, Sci. China Phys. Mech. Astron. **54**, 1367 (2011).
[25] E. Komatsu *et al.*, Astrophys. J. Suppl. Ser. **180**, 330 (2009).
[26] E. Bertschinger, Physica D **77**, 354 (1994).
[27] I. Brevik, S.V. Pettersen, Phys. Rev. D **56**, 3322 (1997).
[28] I.M. Khalatnikov and A.Yu. kamenshchik, Phys. Lett. B **553**, 119 (2003).
[29] G.F.R. Ellis, *Cosmological models*, (2002).
[30] V. Fayaz, H. Hossienkhani, M. Amirabadi and N. Azimi, Astrophys. Space Sci. **353**, 301 (2014).
[31] H. Hossienkhani, A. Najafi and N. Azimi, Astrophys. Space Sci. **353**, 311 (2014).
[32] H. Hossienkhani and A. Pasqua, Astrophys. Space. Sci. **349**, 39 (2014).
[33] O. Bartolami and F. Gil, Phys. Lett. B **654**, 165 (2007).
[34] R. Bousso, Rev. Mod. Phys. **74**, 825 (2002).
[35] A. Sheykhi, Phys. Rev. D **84**, 107302 (2011).
[36] M. Cataldo, N. Cruz, S. del Campo and S. Lepe, Phys. Lett. B **509**, 138 (2001).
[37] N. Radicella and D. Pavón, JCAP, **10**, 005 (2010).
[38] I. Durán, L. Parisi, Phys. Rev. D **85**, 123538 (2012); W. Zimdahl and D. Pavón, Classical and Quantum Gravity **24**, 22 (2006).
[39] P. Horava, D. Minic, Phys. Rev. Lett. **85**, 1610 (2000).
[40] A. Sen, JHEP **10**, 008 (1999).
[41] E.A. Bergshoeff *et al.*, JHEP **0005**, 009 (2000).
[42] T. Padmanabhan, Phys. Rev. D **66**, 021301 (2002).
[43] E.J. Copeland, M.R. Garousi, M. Sami and S. Tsujikawa, Phys. Rev. D **71**, 043003 (2005).
[44] F. Piazza and S. Tsujikawa, JCAP **07**, 004 (2004).
[45] T. Chiba, T. Okabe, M. Yamaguchi, Phys. Rev. D **62**, 023511 (2000).
[46] B. Wang, J. Zang, Ch.Y. Lin, E. Abdalla, S. Micheletti, Nucl. Phys. B **778**, 69 (2007).
[47] M. Li, X.D. Li, S. Wang and X. Zhang, JCAP **0906**, 036 (2009).
[48] J.F. Zhang, Y.H. Li and X. Zhang, Eur. Phys. J. C **73**, 2280 (2013).
[49] T.M. Davis *et al.*, Astrophys.J. **666**, 716 (2007).
[50] J. Zhang, L. Zhang and X. Zhang, Phys. Lett. B **691** , 11 (2010).
[51] R.Y. Guo and X. Zhang, Eur. Phys. C **76**, 163 (2016).
[52] J. Simon, L. Verde and R. Jimenez, Phys. Rev. D **71**, 123001 (2005).
[53] M. Moresco, Mon. Not. R. Astron. Soc. **450**, L16 (2015).
[54] R. Jimenez, Rom. Journ. Phys. **5**, 863 (2012).
[55] C. Blake *et al.*, Mon. Not. R. Astron. Soc. **425**, 405 (2012); Y.L. Li, S.Y. Li, T.J. Zhang and T.P. Li, Astrophys. J. **789**, L15 (2014).

[56] P.K. Aluri, S. Panda, M. Sharma, S. Thakur, JCAP, **12**, 003 (2013).
[57] D.N. Spergel, R. Bean, O. Doré *et al.*, Astrophys. J. Suppl. **170**, 377 (2007).
[58] J.R. Gott, M.S. Vogeley, S. Podariu and B. Ratra, Astrophys. J. **549**, 1 (2001).
[59] J. Liske, A. Grazian, E. Vanzella, M. Dessauges *et al.*, Mon. Not. Roy. Astron. Soc. **386**, 1192 (2008).
[60] X. Zhang, Phys. Rev. D **79**, 103509 (2009).
[61] V. Sahni *et al.*, JETP Lett. **77**, 201 (2003).
[62] U. Alam, V. Sahni, T.D. Saini and A.A. Starobinsky, MNRAS, **344**, 1057 (2003).
[63] F.Y. Wang, Z.G. Dai and S. Qi, Astronomy & Astrophysics **507**, 53 (2009).
[64] S. Chattopadhyay, Mod. Phys. Lett. A **31**, 1650202 (2016).
[65] F. Pace, L. Moscardini, R. Crittenden, M. Bartelmann, V. Pettorino, MNRAS **437**, 547 (2014).
[66] W.J. Percival, A & A **443**, 819 (2005).
[67] S. Wang, Y. Wang and M. Li, (2016), arXiv:1612.00345v1.
[68] A.G. Riess, W.H. Press, R.P. Kirshner, ApJ, **473**, 588 (1996).
[69] A.G. Riess, L.G. Strolger, S. Casertano *et al.*, ApJ, **659**, 98 (2007).
[70] V. Fayaz and H. Hossienkhan, 2016, arXiv:1612.02453.